Mahmmod, BM, Abdulhussain, SH, Suk, T and Hussain, A

Fast Computation of Hahn Polynomials for High Order Moments

IEEE Access
Multidisciplinary ⋮ Rapid Review ⋮ Open Access Journal

Received April 6, 2022, accepted April 22, 2022, date of publication April 28, 2022, date of current version May 11, 2022.

Digital Object Identifier 10.1109/ACCESS.2022.3170893

Fast Computation of Hahn Polynomials for High Order Moments

BASHEERA M. MAHMMOD[1], SADIQ H. ABDULHUSSAIN[1], TOMÁŠ SUK[2], (Member, IEEE), AND ABIR HUSSAIN[3,4], (Member, IEEE)

[1]Department of Computer Engineering, University of Baghdad, Baghdad 10071, Iraq
[2]Institute of Information Theory and Automation, Czech Academy of Sciences, 182 08 Prague, Czech Republic
[3]School of Computer Science and Mathematics, Liverpool John Moores University, Liverpool L3 3AF, U.K.
[4]Department of Electrical Engineering, University of Sharjah, Sharjah, United Arab Emirates

Corresponding author: Abir Hussain (a.hussain@ljmu.ac.uk)

This work was supported in part by the Czech Science Foundation under Grant GA21-03921S, and in part by the Praemium Academiae.

ABSTRACT Discrete Hahn polynomials (DHPs) and their moments are considered to be one of the efficient orthogonal moments and they are applied in various scientific areas such as image processing and feature extraction. Commonly, DHPs are used as object representation; however, they suffer from the problem of numerical instability when the moment order becomes large. In this paper, an operative method to compute the Hahn orthogonal basis is proposed and applied to high orders. This paper developed a new mathematical model for computing the initial value of the DHP and for different values of DHP parameters (α and β). In addition, the proposed method is composed of two recurrence algorithms with an adaptive threshold to stabilize the generation of the DHP coefficients. It is compared with state-of-the-art algorithms in terms of computational cost and the maximum size that can be correctly generated. The experimental results show that the proposed algorithm performs better in both parameters for wide ranges of parameter values α and β, and polynomial sizes.

INDEX TERMS Hahn polynomials, Hahn moments, propagation error, numerical error.

I. INTRODUCTION

Moment theory and its variants are significant tools in imaging and computer vision applications [1]–[3]. Moments are scalar quantities used for characterization of the signal. Moments are obtained by using a set of polynomial basis functions. They are used to transform signal from time domain (such as speech) or spatial domain (such as image) into the transform domain [4], [5]. Geometric moments and moments invariants were introduced by [6] to deal with the problem of pattern recognition. They are not orthogonal [7], what causes numerical problems.

Continuous moments are obtained using continuous orthogonal polynomials (COPs), e.g. Zernike [8], [9] or Chebyshev with transformed radius [10]. Continuous moment functions are inaccurate because of two sources of errors: coordinate transformation of the image and the approximation of the continuous integral [11]. As a result, during image reconstruction process, the image will be far from perfect due to discretization and approximation [12].

The associate editor coordinating the review of this manuscript and approving it for publication was P. K. Gupta.

In order to surmount these shortcomings, researches oriented towards discrete orthogonal polynomials (DOPs). They show better capabilities in image reconstruction [11]–[13]. Beside, discrete orthogonal moments (DOMs) have the ability to represent 1D and 2D signals without redundancy, high energy compaction, and spectral resolution properties [14]–[17]. Several types of DOPs have been recently used for signal representation and feature extraction such as discrete Chebyshev polynomials [18], [19], discrete Krawtchouk moments [20], [21], and discrete Hahn moments [22]. In addition, DOPs are used to solve linear functional differential equations [23].

The robustness of DOPs is essentially based on some important properties such as energy compaction, efficient data processing, numerical stability, robust data analysis, extraction features from the signal, and localization [5], [24]. However, the remarkable properties of the most DOMs can be applied only to medium size images, they are not applicable for large size images or high moment orders [25]. This limitation is determined by the DOP overflow, fluctuation of the polynomial values, as well as the high computational cost. Thus, new recurrence algorithms for generating the

higher orders are still developed, e.g. for Chebyshev [19] and Krawtchouk [20] polynomials. Recently, researchers have discussed other DOPs such as Charlier polynomials [26] and Hahn polynomials [25].

The recursive algorithms reduce the complexity of calculating the coefficients of DOPs and the propagation of errors [27], [28]. We can use either a single recursive formula with respect to degree n or a double recursive formula also with respect to spacial or time coordinate x. The problem of numerical instability is solved by calculating the DOP coefficients with respect to the variable n. However, this calculation is not efficient, when the size of 1D or 2D signals becomes large. For instance, the coefficients of Chebyshev polynomials have numerical instabilities since the squared norm of the scaled Chebyshev polynomials assumes small values. Mukundan [12] propoesed the recurrence algorithm in the x-direction to resolve this issue. After that, many researches began to work on this problem such as [27].

In general, an attention has been paid to the computation cost, which is considered to be an important point that subjects to ill-conditioning, therefore it is taking a substantial consideration in different researches [29], [30]. For Meixner moment coefficients, this drawback is resolved via fast and efficient calculation in [31]. For Chebyshev moments, a fast and stable method is proposed by Abdulhussain *et al.* [19] for higher polynomial degree by a combination of the three-term recurrence relations in the n- and x-directions. Daoui *et al.* [25] proposed a new method using a modified Gram-Schmidt orthogonalization process. This method reduces the numerical error propagation during recursive computations. However, it is relatively slow.

Motivated by this problem for the discrete orthogonal Hahn moments, this study introduces a new algorithm to tackle this issue through composing two recurrence algorithms (n- and x-recurrence relations) and an adaptive threshold to stabilize the generation of the DHP coefficients. Our main contribution are as follows:

1) A stable computation of initial values is proposed.
2) A double recurrence both in order and in coordinate are proposed.
3) A condition is utilized to prevent underflow in high orders.
4) The proposed algorithm for Hahn polynomials preserves the orthogonality condition for large signal sizes as well as higher orders.

The present paper is organized as follows: in Section II, the preliminaries and the existed three-term recurrence algorithms are presented. In Section III, the proposed recurrence algorithm is presented. In Section IV, the experimental analysis is performed to evaluate the proposed recurrence algorithm. Finally, conclusions are drawn in Section V.

II. PRELIMINARIES

The mathematical definitions and fundamentals of DHP and discrete Hahn moments (DHMs) are introduced in this section.

A. THE MATHEMATICAL DEFINITION OF DHP

DHPs of the nth degree $\mathcal{H}_n^{\alpha,\beta}(x)$ are defined as the solution of the difference relation [27], [32], which is given by

$$\phi(x)\Delta\nabla\mathcal{H}_n^{\alpha,\beta}(x) + \psi(x)\Delta\mathcal{H}_n^{\alpha,\beta}(x) + \lambda_n\mathcal{H}_n^{\alpha,\beta}(x) = 0, \quad (1)$$

where $\phi(x)$ and $\psi(x)$ are first and second order functions, respectively, and λ_n is a constant. $\Delta\mathcal{H}_n^{\alpha,\beta}(x)$ and $\nabla\mathcal{H}_n^{\alpha,\beta}(x)$ represent the forward and backward difference, respectively. The values of $\phi(x)$, $\psi(x)$, and λ_n are defined as follows [27]

$$\phi(x) = x(N+\alpha-x) \quad (2)$$
$$\psi(x) = (\beta+1)(N-1) - (\alpha+\beta+2)x \quad (3)$$
$$\lambda_n = n(\alpha+\beta+n+1), \quad (4)$$

where α and β are the DHP parameters (α and $\beta > -1$ or also α and $\beta < -N$). The values of $\Delta\mathcal{H}_n^{\alpha,\beta}(x)$ and $\nabla\mathcal{H}_n^{\alpha,\beta}(x)$ are defined as follows

$$\Delta\mathcal{H}_n^{\alpha,\beta}(x) = \mathcal{H}_n^{\alpha,\beta}(x+1;N) - \mathcal{H}_n^{\alpha,\beta}(x;N) \quad (5)$$
$$\nabla\mathcal{H}_n^{\alpha,\beta}(x) = \mathcal{H}_n^{\alpha,\beta}(x;N) - \mathcal{H}_n^{\alpha,\beta}(x-1;N). \quad (6)$$

From Eqs. (5) and (6), $\Delta\nabla\mathcal{H}_n^{\alpha,\beta}(x)$ can be written

$$\Delta\nabla\mathcal{H}_n^{\alpha,\beta}(x) = \mathcal{H}_n^{\alpha,\beta}(x+1;N) - 2\mathcal{H}_n^{\alpha,\beta}(x) + \mathcal{H}_n^{\alpha,\beta}(x-1;N), \quad (7)$$

where n represents the polynomial degree, x is the signal index, and N is the polynomial size (the number of samples). The solution of Eq. (1) is

$$\mathcal{H}_n^{\alpha,\beta}(x;N) = \frac{(-1)^n(\beta+1)_n(N-n)_n}{n!} \times {}_3F_2\left(\left.\begin{matrix}-n, -x, n+1+\alpha+\beta\\ \beta+1, 1-N\end{matrix}\right| 1\right), \quad (8)$$

where ${}_3F_2(\cdot)$ represents the generalized hypergeometric series which is given by

$${}_3F_2\left(\left.\begin{matrix}a, b, c\\ d, e\end{matrix}\right| z\right) = \sum_{k=0}^{\infty}\frac{(a)_k(b)_k(c)_k}{(d)_k(e)_k k!}(z)^k \quad (9)$$

and $(\cdot)_k$ represents the rising factorial also known as Pochhammer symbol. It is given by

$$(a)_k = a(a+1)(a+2)\cdots(a+k-1). \quad (10)$$

DHPs satisfy the orthogonality condition[1] as follows

$$\sum_{x=0}^{N-1}\mathcal{H}_n^{\alpha,\beta}(x;N)\,\mathcal{H}_m^{\alpha,\beta}(x;N)\,\omega_{\mathcal{H}}(x) = \rho_{\mathcal{H}}(n)\delta_{nm} \quad (11)$$

where δ_{nm} represents the Kronecker delta, $\omega_{\mathcal{H}}$ and $\rho_{\mathcal{H}}$ are the weight and norm functions of DHP

$$\omega_{\mathcal{H}}(x) = \frac{\Gamma(N+\alpha-x)\Gamma(\beta+x+1)}{\Gamma(N-x)\Gamma(x+1)} \quad (12)$$
$$\rho_{\mathcal{H}}(n) = \frac{\Gamma(\alpha+n+1)\Gamma(\beta+n+1)(\alpha+\beta+n+1)_N}{(2n+\alpha+\beta+1)\Gamma(n+1)\Gamma(N-n)}. \quad (13)$$

[1] We can find alternative definition with different range of the orthogonality from 0 to N [33] instead of that from 0 to $N-1$ in (11). Then, all other formulas are modified.

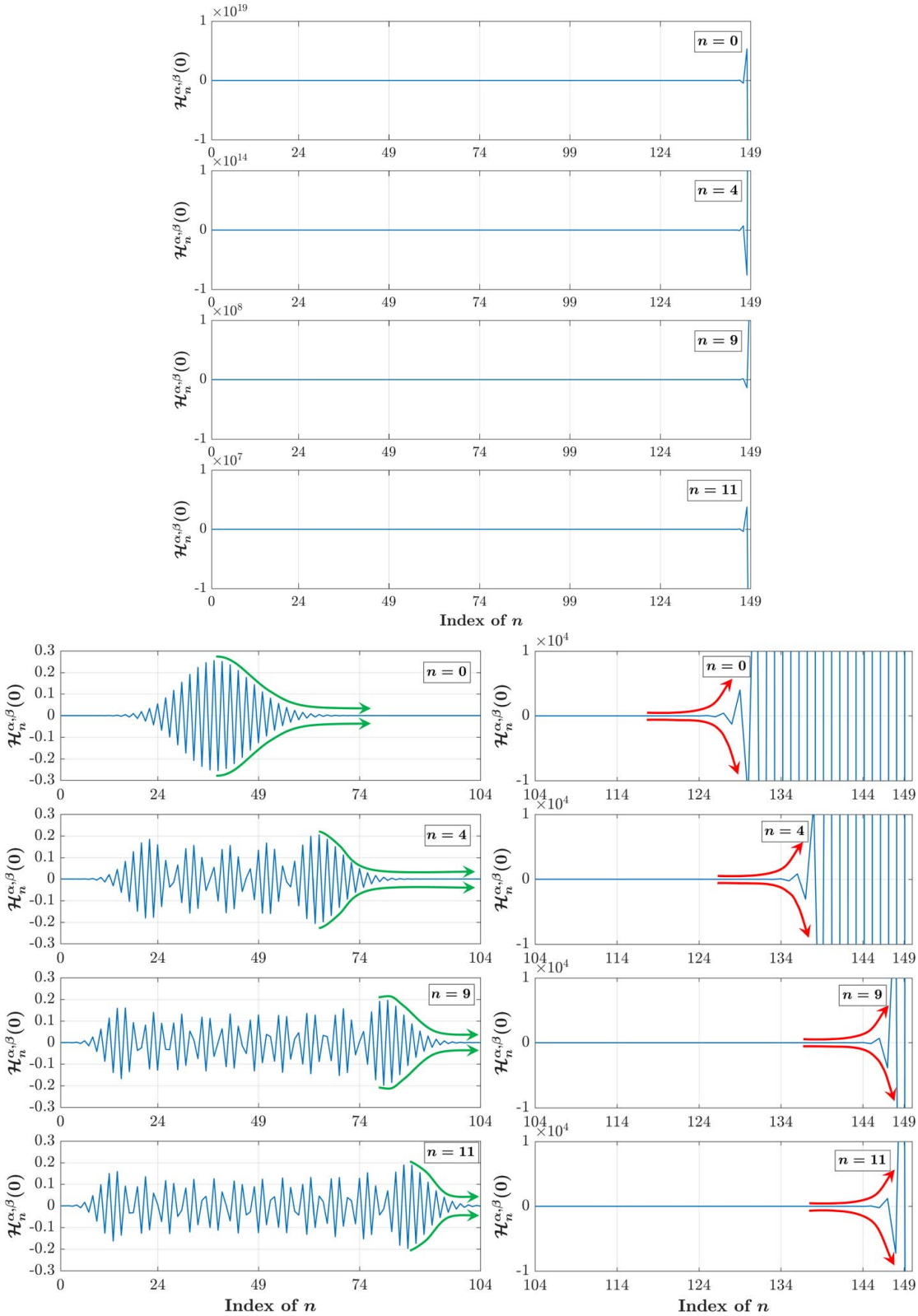

FIGURE 1. Plot of DHP with different degree and a size of 150. Top row shows entire $\hat{\mathcal{H}}_n^{\alpha,\beta}(0;N)$, bottom left shows stable values in the range of $n = 0, 1, \ldots, 104$, and bottom right column shows unstable values and the starting point of instability due to numerical errors in the range $n = 104, 105, \ldots, 149$. Note: the green arrow represents stable values of DHP coefficients, while the red arrow represents unstable values.

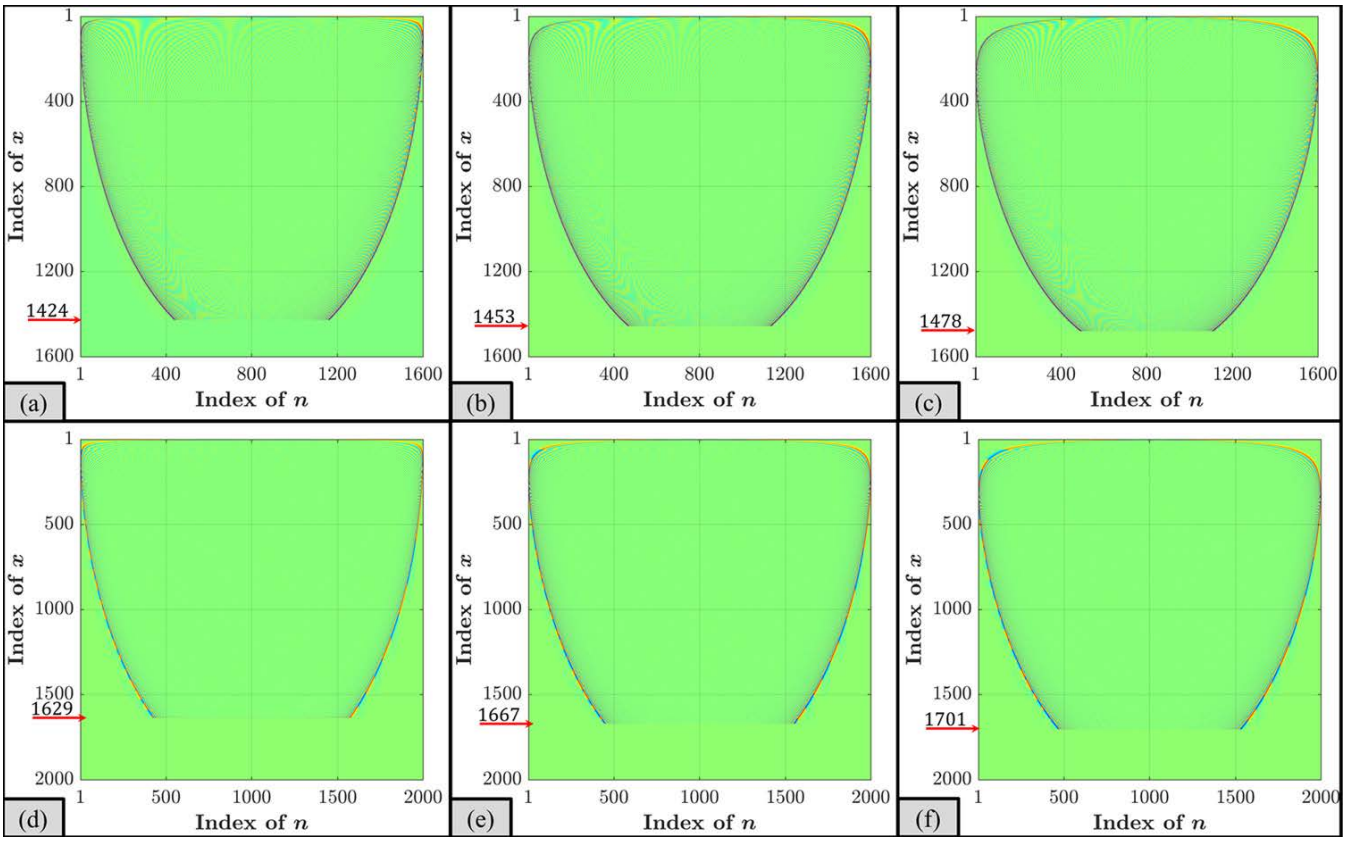

FIGURE 2. 2D plots of the DHP. (a) $N = 1600$ and $\alpha = \beta = 10$, (b) $N = 1600$ and $\alpha = \beta = 40$, (c) $N = 1600$ and $\alpha = \beta = 80$, (d) $N = 2000$ and $\alpha = \beta = 10$, (e) $N = 2000$ and $\alpha = \beta = 40$, and (f) $N = 2000$ and $\alpha = \beta = 80$.

The weighted DHP of nth degree is given by

$$\hat{\mathcal{H}}_n^{\alpha,\beta}(x;N) = \mathcal{H}_n^{\alpha,\beta}(x;N)\sqrt{\frac{\omega_{\mathcal{H}}}{\rho_{\mathcal{H}}}}. \tag{14}$$

B. THE DEFINITION OF DHM

DHMs are the signal (speech or images) projection on the DHP basis. For two-dimensional signal (image), $f(x, y)$, the DHMs, η_{nm}, is computed as follows

$$\eta_{nm} = \sum_{x=0}^{N_1-1}\sum_{y=0}^{N_2-1} \hat{\mathcal{H}}_n^{\alpha,\beta}(x;N_1)\,\hat{\mathcal{H}}_m^{\alpha,\beta}(y;N_2)\,f(x,y)$$
$$n = 0, 1, \ldots, N_1 - 1; \quad \text{and} \quad m = 0, 1, \ldots, N_2 - 1, \tag{15}$$

where $N_1 \times N_2$ is the size of the image $f(x, y)$. The image can be reconstructed from Hahn moment domain into the spatial domain by

$$\hat{f}(x,y) = \sum_{n=0}^{N_1-1}\sum_{m=0}^{N_2-1} \hat{\mathcal{H}}_n^{\alpha,\beta}(x;N_1)\,\hat{\mathcal{H}}_n^{\alpha,\beta}(y;N_2)\,\eta_{nm}$$
$$x = 0, 1, \ldots, N_1 - 1; \quad \text{and} \quad y = 0, 1, \ldots, N_2 - 1. \tag{16}$$

C. EXISTING RECURRENCE ALGORITHMS

The three term recurrence relations are employed because of both the time consumption and the insufficient precision of the hypergeometric series in Eq. (8). In this section, the existing recurrence algorithms and their analysis are briefly presented.

1) THE THREE TERM RECURRENCE RELATION IN THE n-DIRECTION (TTRRnd)

The DHP of the nth degree at the xth index is given by [27]

$$\hat{\mathcal{H}}_n^{\alpha,\beta}(x;N) = \frac{\mathcal{AB}}{\mathcal{E}}\hat{\mathcal{H}}_{n-1}^{\alpha,\beta}(x;N) + \frac{\mathcal{CD}}{\mathcal{E}}\hat{\mathcal{H}}_{n-2}^{\alpha,\beta}(x;N)$$
$$n = 2, 3, \ldots, N-1; \quad \text{and} \quad x = 0, 1, \ldots, N-1, \tag{17}$$

where the parameters of the n-direction recurrence algorithms are (18), as shown at the bottom of the next page, with initial values

$$\hat{\mathcal{H}}_0^{\alpha,\beta}(x;N) = \sqrt{\frac{\omega_{\mathcal{H}}(x)}{\rho_{\mathcal{H}}(0)}} \tag{19}$$

$$\hat{\mathcal{H}}_1^{\alpha,\beta}(x;N) = [-(\beta+1)(N-1) + x(\alpha+\beta+2)] \times \sqrt{\frac{\omega_{\mathcal{H}}(x)}{\rho_{\mathcal{H}}(1)}}. \tag{20}$$

The limitation of the n-direction recurrence algorithm arises from the initial values $\hat{\mathcal{H}}_0^{\alpha,\beta}(x;N)$ and $\hat{\mathcal{H}}_1^{\alpha,\beta}(x;N)$. They are bounded to limited polynomial size N and DHP

parameters α and β. The maximum polynomial size that can be generated is 135 samples, when DHP parameters, α and β, are 20 and 20, respectively. The limitation arises from the nature of the formula used. Although this issue can be solved by reducing the complexity of the formula employed to compute the values of the initial sets, the n-direction recurrence algorithm still suffers from the numerical propagation error. It is taken place when the values of the DHP coefficients (DHPCs) decrease in their values as shown in FIGURE 1.

2) THE THREE TERM RECURRENCE RELATION IN THE x-DIRECTION (TTRRxd)

DHP of nth degree at the xth index is computed as [27]

$$\begin{aligned}&\hat{\mathcal{H}}_n^{\alpha,\beta}(x;N)\\&\quad=\eta_1\left[\eta_2\hat{\mathcal{H}}_n^{\alpha,\beta}(x-1;N)+\eta_3\hat{\mathcal{H}}_n^{\alpha,\beta}(x-2;N)\right]\\&x=2,3,\ldots,N-1;\quad\text{and}\quad n=0,1,\ldots,N-1,\end{aligned}\tag{21}$$

where the coefficients of the x-direction recurrence algorithm are (22), as shown at the bottom of the next page, with initial values

$$\hat{\mathcal{H}}_n^{\alpha,\beta}(0;N)=(1-N)_n\binom{n+\beta}{n}\sqrt{\frac{\omega_{\mathcal{H}}(0)}{\rho_{\mathcal{H}}(n)}}\tag{23}$$

$$\begin{aligned}\hat{\mathcal{H}}_n^{\alpha,\beta}(1;N)=&\frac{(n+\beta+1)(N-n-1)-n(N+\alpha-1)}{(\beta+1)(N-1)}\\&\times\sqrt{\frac{\omega_{\mathcal{H}}(1)}{\omega_{\mathcal{H}}(0)}}\hat{\mathcal{H}}_n^{\alpha,\beta}(0;N).\end{aligned}\tag{24}$$

To reduce the time required to compute the DHPCs, the following symmetry relation [25] is employed

$$\hat{\mathcal{H}}_n^{\alpha,\beta}(x;N)=(-1)^n\hat{\mathcal{H}}_n^{\alpha,\beta}(N-1-x;N)\ \text{ for } \alpha=\beta.\tag{25}$$

Using the symmetry relation, Eq. (25) reduces the computed coefficients to 50%. However, there are two limitations in the recurrence relation in the x-directions as follows: 1) the initial set $\hat{\mathcal{H}}_n^{\alpha,\beta}(0;N)$ becomes zero when the number of samples or the parameter values becomes too big because of the nature of the formula used in Eq. (23), and 2) the coefficient values become underflowed as the degree of the polynomial becomes large; this is because of the initial values becomes less than 10^{-324}, which becomes zero in various environments, such as Matlab and C++. FIGURE 2 shows DHP using different values of parameters α and β as well as polynomial size using the recurrence relation in the x-direction.

From FIGURE 2, the DHPCs become zero as the polynomial degree increases. For instance, the maximum non-zero coefficients occurred at $n=1423$ when $N=1600$ and $\alpha=\beta=10$ (see FIGURE 2a).

3) RECURRENCE RELATION BASED ON GRAM-SCHMIDT ORTHONORMALIZATION PROCESS (RRGSOP)

Recently, Daoui *et al.* [25] presented an algorithm based on Gram-Schmidt orthonormalization process (GSOP) and the n-direction recurrence relation to compute DHP. The GSOP is used to overcome the problem of the instability in the DHPCs. The presented algorithm begins with the computation of the initial sets $\hat{\mathcal{H}}_0^{\alpha,\beta}(x;N)$ and $\hat{\mathcal{H}}_1^{\alpha,\beta}(x;N)$. Then, the recurrence relation in the n-direction is employed to compute the coefficients for $n>1$. Finally, the GSOP is applied to minimize the numerical errors generated by the n-direction recurrence algorithm. However, the GSOP-based recurrence algorithm satisfies the orthogonality condition, it has three drawbacks. First, the algorithm is not able to correctly generate the coefficients of the DHP when $\alpha\neq\beta$, which is observed from the results in [25]. Second, the algorithm is unable to generate DHP for a broad range of parameters α and β because of the formula utilized to compute the initial values. Third, the GSOP-based recurrence algorithm has high computational cost due to the nested loops of the employed GSOP to minimize the error for each polynomial degree, which in turn increases the number of operations required to compute the coefficients of the DHP.

$$\begin{aligned}\mathcal{A}&=x-\frac{\alpha-\beta+2N-2}{4}-\frac{(-\alpha^2+\beta^2)(\alpha+\beta+2N)}{4(\alpha+\beta+2n-2)(\alpha+\beta+2n)}\\\mathcal{B}&=\sqrt{\frac{n(\alpha+\beta+n)(\alpha+\beta+2n+1)}{(N-n)(\alpha+n)(\beta+n)(\alpha+\beta+2n-1)(\alpha+\beta+N+n)}}\\\mathcal{C}&=-\frac{(\alpha+n-1)(\beta+n-1)(\alpha+\beta+N+n-1)(N-n+1)}{(\alpha+\beta+2n-2)(\alpha+\beta+2n-1)}\\\mathcal{D}&=\sqrt{\frac{n(n-1)(\alpha+\beta+n)(\alpha+\beta+n-1)(\alpha+\beta+2n+1)}{(\alpha+n)(\alpha+n-1)(\beta+n)(\beta+n-1)(N-n+1)(N-n)}}\\&\quad\times\sqrt{\frac{1}{(\alpha+\beta+2n-3)(\alpha+\beta+N+n)(\alpha+\beta+N+n-1)}}\\\mathcal{E}&=\frac{n(\alpha+\beta+n)}{(\alpha+\beta+2n-1)(\alpha+\beta+2n)}\end{aligned}\tag{18}$$

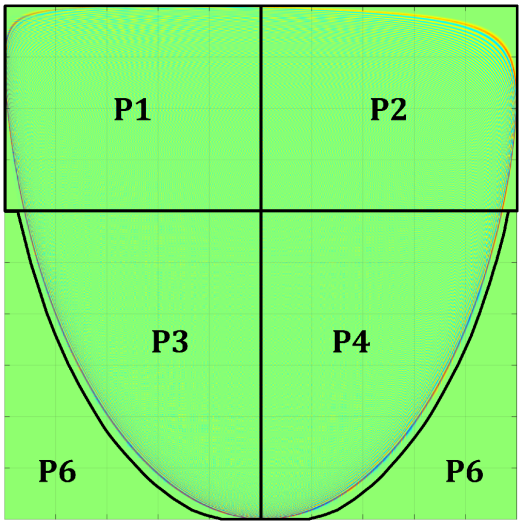

FIGURE 3. Schematic diagram of the proposed algorithm. In parts P1 and P2, the recurrences in the x-direction are utilized, while in parts P3 and P4 the recurrences in the n-directions are utilized. In P6, a stabilizing condition is utilized to prevent underflow in high orders.

III. PROPOSED RECURRENCE ALGORITHM

In this section, the design of the proposed algorithm is presented. For simplicity DHP $\hat{\mathcal{H}}_n^{\alpha,\beta}(x;N)$ is denoted as $\hat{\mathcal{H}}_n^{\alpha,\beta}(x)$. FIGURE 3 shows DHP for $\alpha \neq \beta$, which is considered to be more general than the case $\alpha = \beta$. The plane of the DHP is partitioned into four parts labeled as P1, P2, P3, and P4. In parts P1 and P2, the recurrence in the x-direction are utilized. While, in parts P3 and P4, the recurrence in the n and x-directions are utilized. In addition, a stabilizing condition is utilized to prevent underflow in high orders in parts P3 and P4.

A. INITIAL VALUE AND INITIAL SETS

The initial values are crucial and prerequisite for computation of the DHPC values. The existing algorithms (TTRRnd, TTRRxd, and RRGSOP) compute the initial sets. While TTRRnd and RRGSOP utilize Eqs. (19) and (20), TTRRxd utilizes Eqs. (23) and (24) to determine the initial values. These equations are problematic because of the gamma and binomial functions. Thus, infinity (Inf) or not a number (NaN) are occurred in different environments such as C++, python, and MATLAB, i.e., the coefficients of the initial sets are not correctly computed. In addition, the existing algorithm computes the initial sets using the same formula, which in turn leads to increase the computation time.

From Eq. (14), the initial values are

$$\hat{\mathcal{H}}_0^{\alpha,\beta}(0) = \sqrt{\frac{\Gamma(\alpha+\beta+2)\Gamma(N+\alpha)}{\Gamma(\alpha+1)\Gamma(N+\alpha+\beta+1)}} \quad (26)$$

$$\hat{\mathcal{H}}_0^{\alpha,\beta}(N-1) = \sqrt{\frac{\Gamma(\alpha+\beta+2)\Gamma(N+\beta)}{\Gamma(\beta+1)\Gamma(N+\alpha+\beta+1)}}. \quad (27)$$

They cannot be computed for a wide range of polynomial size and parameters, α and β, because of the gamma function $\Gamma(\cdot)$ produces infinity for argument greater than 172 in the standard double precision arithmetics. The gamma function can be written as follows

$$\Gamma(a) = e^{\log\Gamma(a)}, \quad (28)$$

where $\log\Gamma(\cdot)$ represents the logarithmic gamma function [34]. Using Eq. (28), Eqs. (26) and (27) can be expressed in terms of $\log\Gamma(\cdot)$ functions

$$\hat{\mathcal{H}}_0^{\alpha,\beta}(0) = e^{[\log\Gamma(\alpha+\beta+2)+\log\Gamma(N+\alpha)-\log\Gamma(\alpha+1)-\log\Gamma(N+\alpha+\beta+1)]/2} \quad (29)$$

$$\hat{\mathcal{H}}_0^{\alpha,\beta}(N-1) = e^{[\log\Gamma(N+\beta)+\log\Gamma(\alpha+1)-\log\Gamma(\beta+1)-\log\Gamma(N+\alpha)]/2}\,\hat{\mathcal{H}}_0^{\alpha,\beta}(0). \quad (30)$$

These formulas can be used for $\alpha > -1$ and $\beta > -1$. The parameters can also be less than $-N$, i.e. $\alpha < -N$ and $\beta < -N$. Then we must use slightly modified formulas

$$\hat{\mathcal{H}}_0^{\alpha,\beta}(0) = e^{[-\log\Gamma(-\alpha-\beta-1)-\log\Gamma(-N-\alpha+1)+\log\Gamma(-\alpha)+\log\Gamma(-N-\alpha-\beta)]/2} \quad (31)$$

$$\hat{\mathcal{H}}_0^{\alpha,\beta}(N-1) = e^{[-\log\Gamma(-\alpha-\beta-1)-\log\Gamma(-N-\beta+1)+\log\Gamma(-\beta)+\log\Gamma(-N-\alpha-\beta)]/2}. \quad (32)$$

These formulas are used for each part P1 and P2 in FIGURE 3 separately.

It is noteworthy that the initial value $\hat{\mathcal{H}}_0^{\alpha,\beta}(N-1)$ is computed in terms of $\hat{\mathcal{H}}_0^{\alpha,\beta}(0)$, as given in Eq. (30), to reduce the execution time. FIGURE 4 illustrates the plots for the initial values using the proposed algorithm for large polynomial size $N = 8000$ and different values of DHP parameters α and β. From the FIGURE 4, it can be observed that the initial values can be computed without Inf or NaN

$$\eta_1 = \frac{\sqrt{\omega_{\mathcal{H}}(x)}}{\sigma(x-1)+\tau(x-1)} \qquad \sigma(x) = x(N+\alpha-x)$$
$$\eta_2 = \frac{2\sigma(x-1)+\tau(x-1)-\lambda(n)}{\sqrt{\omega_{\mathcal{H}}(x-1)}} \qquad \tau(x) = (\beta+1)(N-1)-x(\alpha+\beta+2)$$
$$\eta_3 = -\frac{\sigma(x-1)}{\sqrt{\omega_{\mathcal{H}}(x-2)}} \qquad \lambda(n) = n(\alpha+\beta+n+1) \quad (22)$$

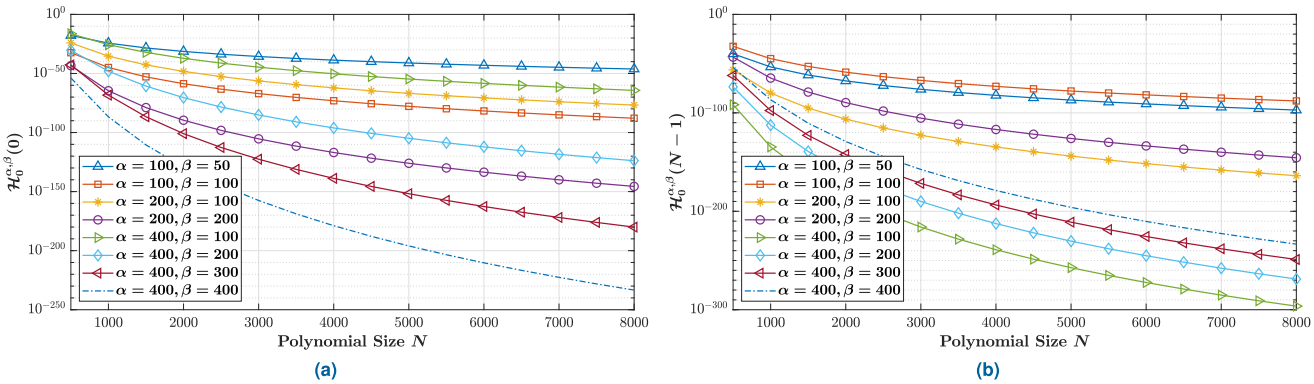

FIGURE 4. Plot of the initial values of DHP coefficients by utilizing the proposed formula for $N = 8000$ and various parameter values of DHP (α and β).

values; thus, the proposed initial formulas for the initial values can be used to compute the rest of the DHPCs.

It is well known that the initial sets are used with the aim of the three term recurrence algorithm for the polynomial computation. The initial sets for part P1 are $\hat{\mathcal{H}}_n^{\alpha,\beta}(0)$ and $\hat{\mathcal{H}}_n^{\alpha,\beta}(1)$ and for part P2 are $\hat{\mathcal{H}}_n^{\alpha,\beta}(N-1)$ and $\hat{\mathcal{H}}_n^{\alpha,\beta}(N-2)$. These sets are computed using two term recurrence algorithm. The initial sets for part P1 are computed as follows

The initial sets for part P2 are computed as follows

B. UTILIZATION OF THE TTRRnd AND TTRRxd IN THE PROPOSED ALGORITHM

The proposed recurrence algorithm is designed on merging the TTRRnd and TTRRxd. For the parts P1 and P2, the coefficients of the DHP are computed using TTRRxd with a maximum degree of 40% of N. For the part P1, the modified TTRRxd (mTTRRxd) is applied as follows

$$\hat{\mathcal{H}}_n^{\alpha,\beta}(x) = (\nu_1+\nu_2)\hat{\mathcal{H}}_n^{\alpha,\beta}(x-1) + \nu_3\hat{\mathcal{H}}_n^{\alpha,\beta}(x-2)$$
$$n = 0, 1, \ldots, M \quad \text{and} \quad x = 2, 3, \ldots, N/2-1, \quad (37)$$

where $M = 0.4N$ to ensure non-zero initial sets. The parameters ν_1, ν_2, and ν_3 of the mTTRRxd are defined by

$$\nu_1 = \frac{-2x^2 + (2N+\alpha-\beta+2)x + (\beta-1)N - \alpha - 1}{\nu}$$
$$\nu_2 = -\frac{n(\alpha+\beta+n+1)}{\nu}$$
$$\nu_3 = -\frac{\sqrt{(\beta+x-1)(N-x+1)(x-1)(N+\alpha-x+1)}}{\nu}$$
$$\nu = \sqrt{(N-x)(\beta+x)(N+\alpha-x)x}. \quad (38)$$

For the part P2, the mTTRRxd is applied backwardly as follows

$$\hat{\mathcal{H}}_n^{\alpha,\beta}(x-2) = \frac{1}{\nu_3}\hat{\mathcal{H}}_n^{\alpha,\beta}(x) - \frac{\nu_1+\nu_2}{\nu_3}\hat{\mathcal{H}}_n^{\alpha,\beta}(x-1)$$
$$n = 0, 1, \ldots, M; \quad \text{and} \quad x = N-2, N-3, \ldots, N/2. \quad (39)$$

After computing the coefficients in parts P1 and P2, the coefficients in parts P3 and P4 are computed using the modified TTRRnd (mTTRRnd) and mTTRRxd.

The coefficients of part P3 are computed in the range $n = M, M+1, \ldots, N-1$ and $x = N/2-1, N/2-2, \ldots, 0$ ($x = (N-1)/2-1, (N-1)/2-2, \ldots, 0$ for odd N) and the coefficients of part P4 are computed in the range $n = M, M+1, \ldots, N-1$ and $x = N/2, N/2+1, \ldots, N-1$ ($x = (N-1)/2, (N-1)/2+1, \ldots, N-1$) as follows

$$\hat{\mathcal{H}}_n^{\alpha,\beta}(x) = \kappa_1\kappa_2\hat{\mathcal{H}}_{n-1}^{\alpha,\beta}(x) + \kappa_3\hat{\mathcal{H}}_{n-2}^{\alpha,\beta}(x). \quad (40)$$

The parameters κ_1, κ_2, and κ_3 of the mTTRRxd are defined by (41), as shown at the bottom of the next page

For each computed coefficient at the xth index in parts P3 and P4, when the previously computed coefficient is less than the currently computed coefficient and less then 10^{-6}, the mTTRRxd is stopped, the rest of the coefficients (part P6) is left zero and the computation continues by the next degree $n+1$.

C. SUMMARY OF THE PROPOSED RECURRENCE ALGORITHM

For more clarification, the procedure of the proposed algorithm for $\alpha \neq \beta$ are shown in FIGURE 5 and can be summarized as follows:

Step 1: Compute the initial values $\hat{\mathcal{H}}_0^{\alpha,\beta}(0)$ and $\hat{\mathcal{H}}_0^{\alpha,\beta}(N-1)$ using Eqs. (29) and (30), respectively. (Eqs. (31) and (32) respectively).

Step 2: Compute the initial sets $\hat{\mathcal{H}}_n^{\alpha,\beta}(0)$ and $\hat{\mathcal{H}}_n^{\alpha,\beta}(1)$ using Eqs. (33) and (34), as shown at the bottom of the next page. The initial sets $\hat{\mathcal{H}}_n^{\alpha,\beta}(N-1)$ and $\hat{\mathcal{H}}_n^{\alpha,\beta}(N-2)$ are computed using Eqs. (35) and (36), as shown at the bottom of the next page.

Step 3: Compute the coefficients of DHP in part P1 using mTTRxd given in Eq. (37), while the coefficients of DHP in part P2 are computed using backward mTTRRxd given in (39).

Step 4: Compute the coefficients of the DHP in parts P3 and P4 using backward mTTRxd given in (40) for the range $n = M+1, M+2, \ldots, N-1$. The coordinate

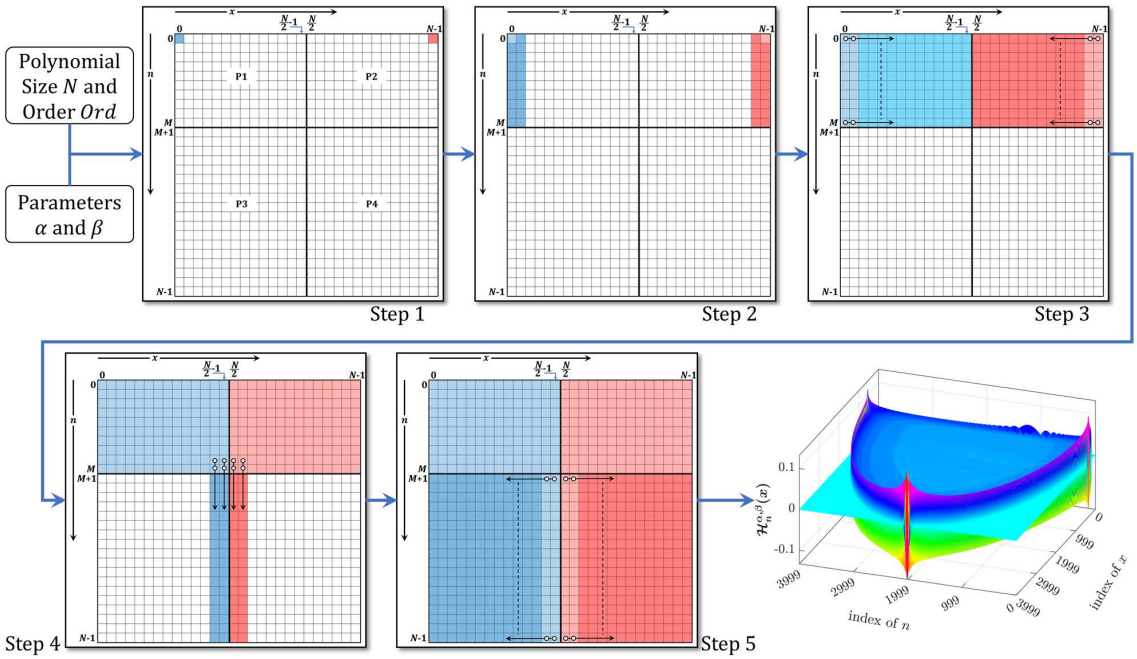

FIGURE 5. Steps of the proposed algorithm.

x in P3 is in the range $x = N2-1, N2-2, \ldots, 0$ and in P4 in the range $x = N2, N2+1, \ldots, N-1$. $N2 = N/2$ for even N and $N2 = (N-1)/2$ for odd N.

$$\hat{\mathcal{H}}_{n+1}^{\alpha,\beta}(0) = -\sqrt{\frac{(n+1+\beta)(N-1-n)(2n+3+\beta+\alpha)(n+\beta+\alpha+1)}{(n+1)(\alpha+1+n)(n+1+\beta+\alpha+N)(2n+\beta+\alpha+1)}}\,\hat{\mathcal{H}}_{n}^{\alpha,\beta}(0), \quad n = 1, 2, \ldots, N-1 \tag{33}$$

$$\hat{\mathcal{H}}_{n}^{\alpha,\beta}(1) = \frac{(N-n-1)\beta - n^2 - (\alpha+1)n + N - 1}{(\beta+1)(N-1)}\sqrt{\frac{(\beta+1)(N-1)}{\alpha+N-1}}\,\hat{\mathcal{H}}_{n}^{\alpha,\beta}(0), \quad n = 0, 1, \ldots, N-1. \tag{34}$$

$$\hat{\mathcal{H}}_{n+1}^{\alpha,\beta}(N-1) = \sqrt{\frac{(2n+3+\alpha+\beta)(n+\alpha+\beta+1)(n+1+\alpha)(N-n-1)}{(n+\beta+1)(n+1+\alpha+\beta+N)(2n+\alpha+\beta+1)(n+1)}}\,\hat{\mathcal{H}}_{n}^{\alpha,\beta}(N-1), \quad n = 1, 2, \ldots, N-1 \tag{35}$$

$$\hat{\mathcal{H}}_{n}^{\alpha,\beta}(N-2) = \frac{-n^2 + (-\alpha-\beta-1)n + (N-1)(\alpha+1)}{\sqrt{(\beta+N-1)(N-1)(\alpha+1)}}\,\hat{\mathcal{H}}_{n}^{\alpha,\beta}(N-1), \quad n = 0, 1, \ldots, N-1. \tag{36}$$

$$\begin{aligned}
\kappa_1 &= (\alpha+\beta+2n)\sqrt{\frac{(\alpha+\beta+2n+1)(\alpha+\beta+2n-1)}{n(\alpha+\beta+n)(N-n)(\alpha+n)(\beta+n)(\alpha+\beta+N+n)}} \\
\kappa_2 &= x - \frac{1}{4}\left[\alpha-\beta+2N-2+\frac{(\beta^2-\alpha^2)(\alpha+\beta+2N)}{(\alpha+\beta+2n-2)(\alpha+\beta+2n)}\right] \\
\kappa_3 &= -\frac{\alpha+\beta+2n}{\alpha+\beta+2n-2}\sqrt{\frac{(n-1)(\alpha+n-1)(\beta+n-1)(N-n+1)}{n(\alpha+\beta+n)(\alpha+n)(\beta+n)(N-n)}} \\
&\quad\times\sqrt{\frac{(\alpha+\beta+n-1)(\alpha+\beta+2n+1)(\alpha+\beta+N+n-1)}{(\alpha+\beta+2n-3)(\alpha+\beta+N+n)}}
\end{aligned} \tag{41}$$

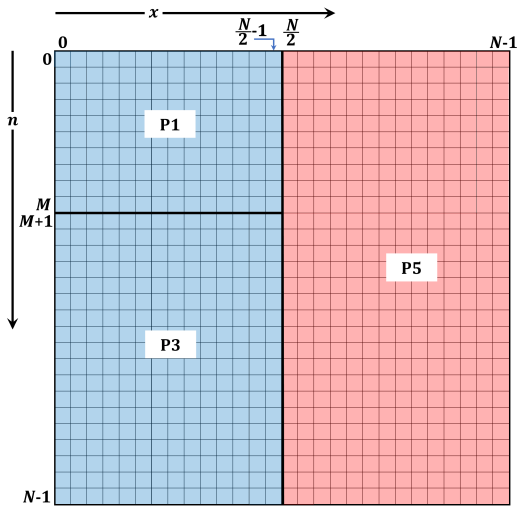

FIGURE 6. Part of the proposed algorithm for $\alpha = \beta$.

Step 5: For each value computed at the xth index, if the absolute value of the previously computed coefficient is less than the currently computed coefficients and less than 10^{-6}, the process is terminated and moved to the next value of n, i.e., $n + 1$. We call the zero coefficients part P6.

It should be noted that for the case of $\alpha = \beta$, the proposed algorithm computes the coefficients in parts P1 and P3, while the coefficients in part P5 are computed using symmetry relation given in Eq. (25).

For more elucidation, the flowchart of the proposed algorithm is shown in FIGURE7

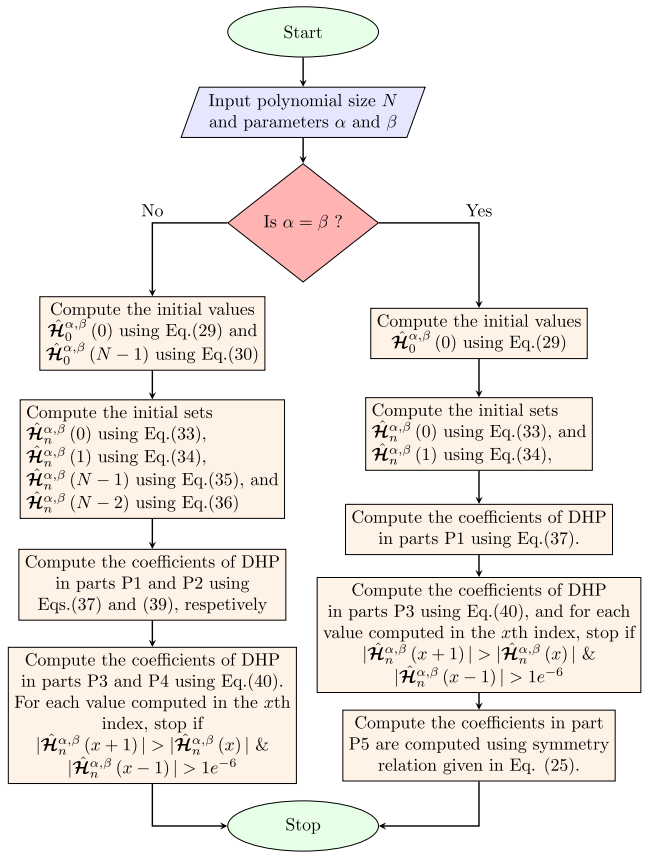

FIGURE 7. Flow chart of the proposed algorithm.

IV. EXPERIMENTAL RESULTS

The performance of the proposed algorithm is evaluated against existing algorithms in this section. The evaluation is performed in terms of the maximum size of the generated polynomial, signal reconstruction, and computational cost. The experiment was carried out using MATLAB environment on MSI-GT60 laptop with a memory of 16GB and core i7-4700MQ CPU.

A. ANALYSIS OF MAXIMUM SIZE

In this experiment, we searched maximum size of DHP generated by the proposed and existing algorithms for various values of parameters α and β. If R is the matrix of values $\hat{\mathcal{H}}_n^{\alpha,\beta}(x)$ with the size $N \times N$, then $R \times R^T$ should be the identity matrix $\mathbb{1}(N)$ of the size $N \times N$. So, mean($|\mathbb{1}(N) - R \times R^T|$) can be used as the average orthogonality error. We searched maximum N satisfying two criteria, average orthogonality error less than 10^{-5} and the computing time less than 1 minute.

The maximum size for each algorithm is reported in TABLE 1. From it we can observe that the proposed algorithm is able to generate DHP with different polynomial parameters without propagation error. The main problem with existing algorithms relies on: 1) the formula used to compute the initial value, and 2) the propagation error generated when the DHPCs becomes very small.

TABLE 1. Comparison between the ability of the proposed algorithm and existing algorithms to generate maximum polynomial size N without propagation error.

α and β	TTRRnd	TTRRxd	RRGSOP	Proposed
$\alpha = 100; \beta = 50$	35	1170	$\emptyset$	9848
$\alpha = 100; \beta = 100$	$\emptyset$	1309	1963	10749
$\alpha = 200; \beta = 100$	$\emptyset$	1213	$\emptyset$	10549
$\alpha = 200; \beta = 200$	$\emptyset$	1414	1963	12037
$\alpha = 400; \beta = 200$	$\emptyset$	1266	$\emptyset$	11624
$\alpha = 400; \beta = 300$	$\emptyset$	1369	$\emptyset$	12907
$\alpha = 400; \beta = 400$	$\emptyset$	1540	1970	14066
$\alpha = 500; \beta = 250$	$\emptyset$	1285	$\emptyset$	8747
$\alpha = 500; \beta = 400$	$\emptyset$	1422	$\emptyset$	11685
$\alpha = 500; \beta = 500$	$\emptyset$	1589	1954	13527

The TTRRnd maximum size is 35 for a very small range of DHP parameters, while the TTRRxd is able to generate a maximum size of 1589 and it works for wide range of the DHP parameters. RRGSOP is able to generate the orthogonal polynomials only when $\alpha = \beta$. The main problem is the time of computation. All results $\neq \emptyset$ cannot be increased because of the time limit 1 minute, while the typical time of computation of the other algorithms is less than 2 s. The proposed algorithm outperforms the existing algorithms in terms of the maximum size and degree that can be generated.

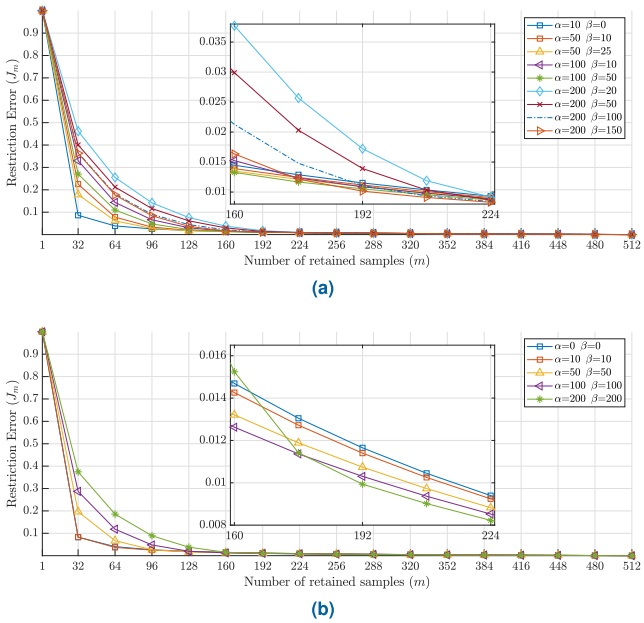

FIGURE 8. Restriction error of DHP (a) for $\alpha \neq \beta$, and (b) $\alpha = \beta$.

FIGURE 9. The image used for the tests.

B. ANALYSIS OF THE ENERGY COMPACTION AND RECONSTRUCTION ERROR

Discrete transforms are dissimilar because of their moments distribution [26]. The sequence of moment indices is essential for the reconstruction of signal information. Therefore, the DHP distribution of the moment energy needs to be investigated before the signal reconstruction analysis. The procedure presented by Jian [35] has been followed to find the distribution of moments. The procedure can be summarized as follows

1) A covariance matrix $\mathcal{CM}$ with length N and zero mean is given by [35]

$$\mathcal{CM} = \begin{bmatrix} 1 & \rho & \rho^2 & \cdots & \rho^{N-1} \\ \rho & 1 & \cdots & \cdots & \vdots \\ \rho^2 & \vdots & \ddots & \vdots & \rho^2 \\ \vdots & \cdots & \cdots & \ddots & \rho \\ \rho^{N-1} & \cdots & \rho^2 & \rho & 1 \end{bmatrix}. \quad (42)$$

2) The covariance matrix $\mathcal{CM}$ is transformed into the discrete Hahn moment domain as follows

$$T = R \times \mathcal{CM} \times R^T, \quad (43)$$

where T is the transformed matrix that is utilized to describe the transform coefficients σ_l^2, and R is the DHP matrix generated with a size of N and degree N.

3) The diagonal coefficients of the matrix T are considered in FIGURE 10.

The aforementioned procedure is carried out using two values of covariance coefficients, $\rho = 0.85$ and $\rho = 0.95$, different values of DHP parameters, and length $N = 16$. The results are reported in TABLE 2. It can inferred from TABLE 2 that the variance values σ_l^2 of the DHP are arranged such that the maximum value is located at $l = 0$ and the variance values reduced as the variance index increased. Thus, the DHP moment order, which is utilized to reconstruct signal information, is given by: $n = 0, 1, \ldots, N-1$.

One of the important properties of the orthogonal-polynomial-based discrete transform is the energy compaction property. This property is employed to measure the tendency of the DHP to reconstruct a large amount of the signal information using a small number of moment coefficients. To examine the impact of the DHP parameters α and β on the energy compaction, the restriction error, $\mathcal{J}$, is used as follows [35]

$$\mathcal{J}_m = \frac{\sum_{a=m}^{N-1} \sigma_a^2}{\sum_{a=0}^{N-1} \sigma_a^2}; \quad m = 0, 1, 2, \ldots, N-1, \quad (44)$$

where σ_a^2 represents σ_l^2 ordered descendingly. FIGURE 8 illustrates the restriction error using covariance coefficient ($\rho = 0.98$) in terms of retained samples q. From FIGURE 8, the DHP parameters, α and β, affect the restriction error. E.g., from FIGURE 8a, when parameter $\alpha = 10$ and $\beta = 0$ shows better energy compaction than other parameter values in the range of $m = 32, \ldots, 96$. However, when $\alpha = 200$ and $\beta = 150$ presents better energy compaction compared to other DHP parameters in the range $m > 192$. On the other hand, FIGURE 8b, the energy compaction for DHP parameters $\alpha = \beta = 0$ and $\alpha = \beta = 10$ shows comparable energy compaction as well as the best energy compaction in the range of retained samples $m = 32, \ldots, 96$. It should be noted that as DHP parameters increases, the energy compaction becomes better in the range of $m > 192$.

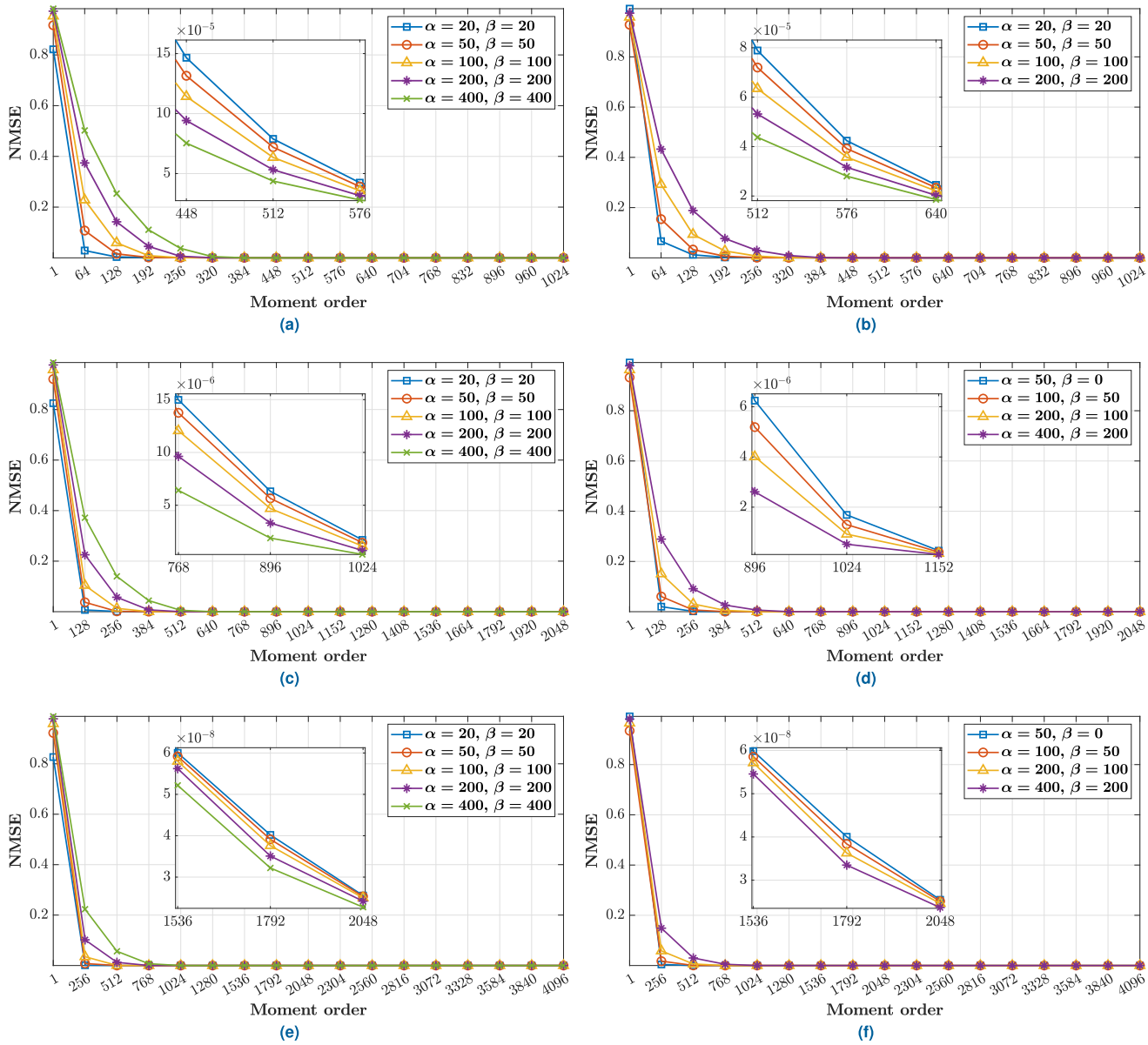

FIGURE 10. NMSE using the proposed algorithm for various parameters values (α and β).

For more evaluation of the proposed algorithm, the normalized mean square error (NMSE) is computed between the image and its reconstructed version. The formula for NMSE, E, is given in [26]

$$E(I, I_r) = \frac{\sum_{x,y} (I(x, y) - I_r(x, y))^2}{\sum_{x,y} (I(x, y))^2} \tag{45}$$

The image "Fruits" shown in FIGURE 9 is used as a test image for reconstruction error analysis. The reconstruction error is performed for different values of DHP parameters, α and β, as well as different polynomial size. For each polynomial size the image is resized accordingly.

First, the reconstruction error analysis is performed for the case of $\alpha = \beta$ as shown in FIGUREs 10a, c, and e and also for the case of $\alpha \neq \beta$ as shown in FIGUREs 10b, d, and f. The image sizes utilized are 1024×1024, 2048×2018, and 4096×4096.

From FIGURE 10, it can be concluded that the proposed algorithm is able to reconstruct the image remarkably for different polynomial size and different values of DHP parameters. It should be noted that when the DHP parameters increase to $\alpha = \beta = 400$, it shows better reconstruction error than other values of DHP parameters. E.g., for image size 4096×4096 , the reconstruction error, NMSE, is reduced to minimum for $\alpha = \beta = 400$, when the number of moments used is greater than 1536×1536. In addition, for the case $\alpha \neq \beta$, the best reconstruction error is occurred at $\alpha = 400$

TABLE 2. Transform coefficient values σ_l^2.

l	ρ=0.85						ρ=0.95					
	α =20 β =20	α =50 β =50	α =100 β =50	α =100 β =100	α =200 β =100	α =200 β =200	α =20 β =20	α =50 β =50	α =100 β =50	α =100 β =100	α =200 β =100	α =200 β =200
0	9.145	8.635	8.031	8.437	7.896	8.331	6.729	6.458	6.121	6.350	6.046	6.292
1	2.713	2.850	2.672	2.886	2.679	2.902	2.622	2.434	2.214	2.359	2.157	2.318
2	1.336	1.255	1.260	1.332	1.291	1.372	2.228	2.267	2.140	2.274	2.135	2.276
3	1.053	1.215	1.141	1.167	1.100	1.142	1.287	1.333	1.291	1.343	1.282	1.347
4	0.676	0.705	0.779	0.711	0.768	0.713	0.986	1.104	1.128	1.148	1.140	1.170
5	0.346	0.472	0.603	0.530	0.638	0.563	0.586	0.673	0.780	0.708	0.793	0.727
6	0.290	0.346	0.527	0.369	0.538	0.380	0.409	0.494	0.633	0.533	0.656	0.555
7	0.107	0.139	0.315	0.162	0.339	0.176	0.253	0.299	0.453	0.323	0.478	0.337
8	0.098	0.136	0.259	0.151	0.289	0.160	0.183	0.211	0.338	0.227	0.363	0.237
9	0.047	0.054	0.144	0.058	0.165	0.061	0.138	0.148	0.237	0.154	0.258	0.159
10	0.041	0.047	0.093	0.051	0.108	0.054	0.117	0.120	0.170	0.123	0.185	0.124
11	0.033	0.034	0.055	0.034	0.062	0.034	0.105	0.104	0.128	0.105	0.135	0.105
12	0.031	0.031	0.038	0.031	0.041	0.031	0.097	0.096	0.105	0.096	0.108	0.096
13	0.029	0.029	0.031	0.029	0.031	0.028	0.091	0.090	0.093	0.090	0.094	0.090
14	0.027	0.027	0.028	0.027	0.028	0.027	0.087	0.086	0.087	0.086	0.087	0.086
15	0.026	0.026	0.026	0.026	0.026	0.026	0.083	0.083	0.083	0.083	0.083	0.083

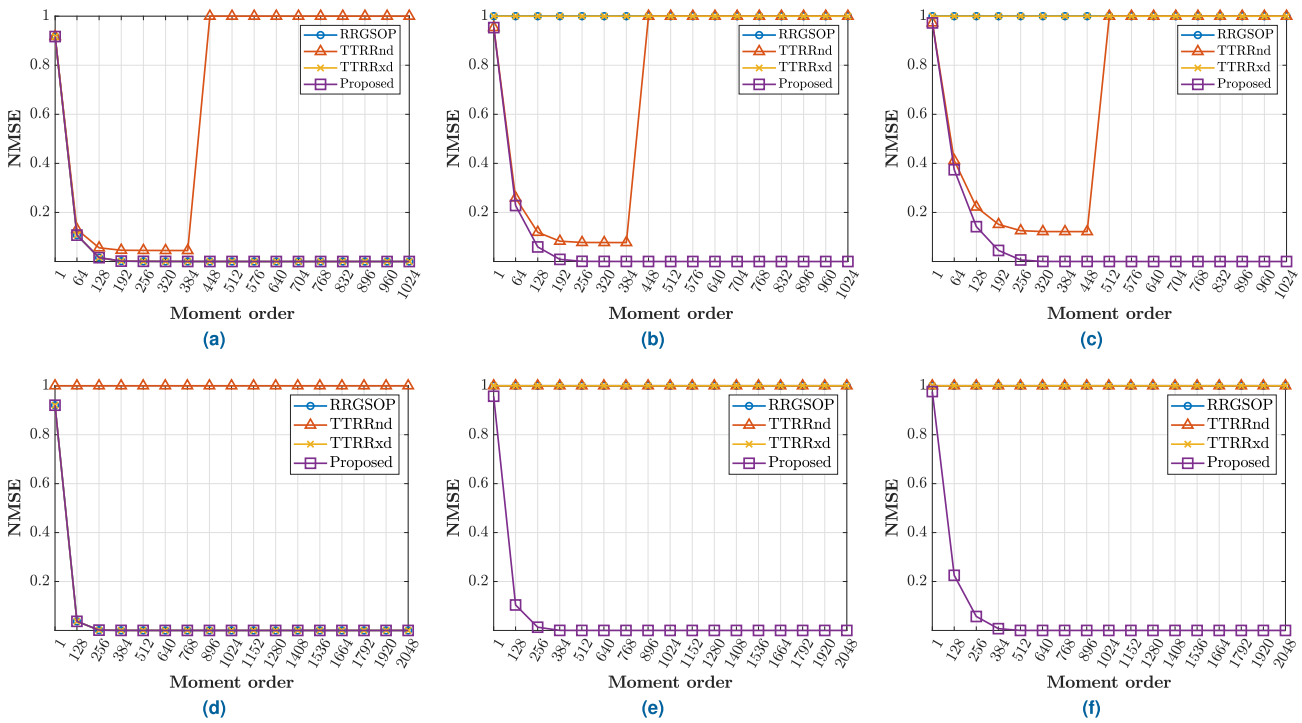

FIGURE 11. Comparison of NMSE between the proposed algorithm and existing works. (a), (b), and (c) image size 1024 × 1024 , (d), (e), and (f) image size 2048 × 2048 , (a) and (d) $\alpha = \beta = 50$, (b) and (e) $\alpha = \beta = 100$, (c) and (f) $\alpha = \beta = 200$.

and $\beta = 200$. For image size of 2048 × 2048, the NMSE declined to minimum for DHP parameters $\alpha = 400$ and $\beta = 200$ before other DHP parameters when the moment matrix used for reconstruction is greater than 896 × 896.

For comparison, the NMSE is computed using the proposed and existing algorithms for different values of DHP parameters and image sizes. FIGUREs 11a, b, and c present the NMSE for image size of 1024 × 1024 with DHP parameters $\alpha = \beta = 50$, $\alpha = \beta = 100$, and $\alpha = \beta = 200$, respectively. In addition, FIGUREs 11d, e, and f illustrate the NMSE for image size of 2048 × 2048 with DHP parameters $\alpha = \beta = 50$, $\alpha = \beta = 100$, and $\alpha = \beta = 200$, respectively. It can be observed that the TTRRnd is unable to reconstruct the image because of the nature of the recurrence algorithm, where the coefficient value of DHP shows high propagation error for all values of DHP parameters, while for TTRRxd, it is able to reconstruct the image for small values of DHP parameters $\alpha = \beta = 50$, as shown in

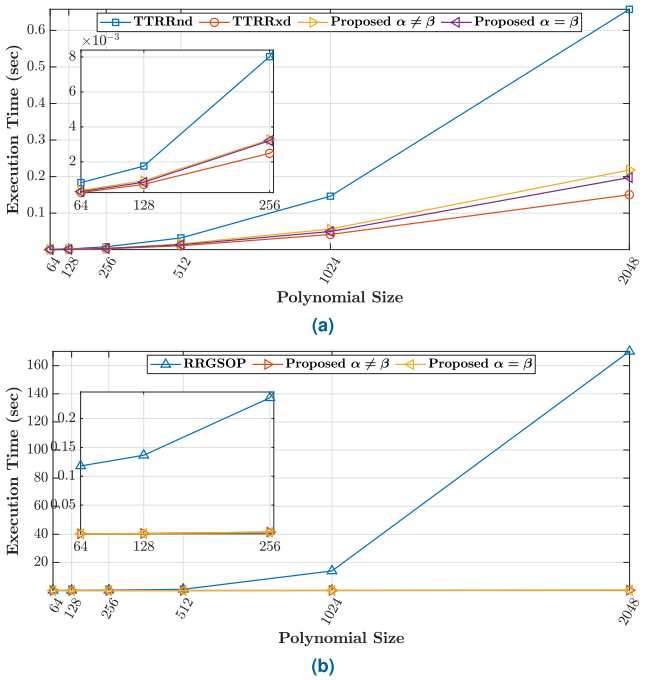

FIGURE 12. Comparison of execution time between the proposed algorithm and existing works.

FIGURE 11a and FIGURE 11d, and unable to reconstruct the image for large values of DHP parameters, as shown in FIGUREs 11b, c, e, and f, where the TTRRxd is unable to generate correct DHPCs for large values of DHP parameters because of the formula used to compute the initial values. Whereas for RRGSOP, the algorithm is able to reconstruct the image correctly as the moment order increases up to $\alpha = \beta = 100$; however, it is unable to reconstruct the image for DHP parameters greater than 100, as shown in FIGURE 11c and FIGURE 11d, because of the formula used to compute the initial values. On the other hand, the proposed algorithm is able to compute DHPCs and to reconstruct the image correctly for different values of DHP parameters and image sizes.

C. COMPUTATIONAL COST ANALYSIS

In this section, the proposed algorithm is evaluated in terms of computational cost. The execution time is performed for the proposed algorithm and compared to that of the existing algorithms. The execution time experiment is carried out using different DHP sizes. It is performed 10 times and the average time for each algorithm is reported as shows in FIGURE 12. It can be observed from FIGURE 12 that the execution time of the proposed algorithm for $\alpha = \beta$ is less than that of the proposed algorithm for $\alpha \neq \beta$ in FIGURE 12a. In addition, the proposed algorithm shows less computation time than that of the TTRRnd because of the proposed algorithm reduces the formula used for computation as depicted in FIGURE 12a. Compared to TTRRxd, the proposed algorithm shows higher execution time than that of the TTRRxd. On the other hand, the execution time required to generate DHP using RRGSOP is higher than that of the proposed algorithm. The average improvement ratio computational cost for the proposed algorithm is ∼0.76, 2.52, and 289.59 over TTRRxd, TTRRnd, and RRGSOP, respectively.

V. CONCLUSION

In this paper, a new recurrence algorithm for DHP is introduced. The proposed algorithm uses the logarithmic gamma function for computation of the initial values so that it is able to compute initial values for different DHP parameters and the large number of samples. The proposed algorithm combines recurrence in degree with recurrence in coordinates and with a condition criterion, so that the propagation error is suppressed. The experiments showed that the proposed algorithm remarkably reduces the computational cost with respect to the existing algorithms. It is able to eliminate propagation errors for large polynomial size and a wide range of DHP parameters. It achieves better signal reconstruction results than other recurrence algorithms for high polynomial degrees.

ACKNOWLEDGMENT

The authors would like to thank the University of Baghdad and LJMU for general and financial support.

REFERENCES

[1] R. N. Hassan, H. S. Ali, and W. H. Wadee, "Computer simulation for the effects of optical aberrations on solar images using Karhunen–Loeve polynomials," *Iraqi J. Sci.*, vol. 62, no. 7, pp. 2463–2473, 2021.

[2] S. H. Abdulhussain, S. A. R. Al-Haddad, M. I. Saripan, B. M. Mahmmod, and A. Hussien, "Fast temporal video segmentation based on Krawtchouk–Tchebichef moments," *IEEE Access*, vol. 8, pp. 72347–72359, 2020.

[3] J. Flusser, T. Suk, and B. Zitová, *2D and 3D Image Analysis by Moments*. Chichester, U.K.: Wiley, 2016.

[4] I. M. Hameed, S. H. Abdulhussain, and B. M. Mahmmod, "Content-based image retrieval: A review of recent trends," *Cogent Eng.*, vol. 8, no. 1, Jan. 2021, Art. no. 1927469. [Online]. Available: https://www.tandfonline.com/doi/full/10.1080/23311916.2021.1927469

[5] B. M. Mahmmod, A. R. B. Ramli, S. H. Abdulhussain, S. A. R. Al-Haddad, and W. A. Jassim, "Signal compression and enhancement using a new orthogonal-polynomial-based discrete transform," *IET Signal Process.*, vol. 12, no. 1, pp. 129–142, Aug. 2018.

[6] M.-K. Hu, "Visual pattern recognition by moment invariants," *IRE Trans. Inf. Theory*, vol. 8, no. 2, pp. 179–187, Feb. 1962.

[7] H. Zhu, H. Shu, J. Zhou, L. Luo, and J.-L. Coatrieux, "Image analysis by discrete orthogonal dual Hahn moments," *Pattern Recognit. Lett.*, vol. 28, no. 13, pp. 1688–1704, 2007.

[8] A.-W. Deng, C.-H. Wei, and C.-Y. Gwo, "Stable, fast computation of high-order Zernike moments using a recursive method," *Pattern Recognit.*, vol. 56, pp. 16–25, Aug. 2016.

[9] L. K. Abood, S. M. Al-Hilly, and R. N. Hassan, "Describing the wavefront aberrations of the hexagonal aperture using modified Zernike polynomials," *Iraqi J. Sci.*, vol. 54, no. 1, pp. 222–231, 2013.

[10] K. M. Hosny and M. M. Darwish, "New set of multi-channel orthogonal moments for color image representation and recognition," *Pattern Recognit.*, vol. 88, pp. 153–173, Apr. 2019.

[11] R. Mukundan, S. H. Ong, and P. A. Lee, "Discrete vs. continuous orthogonal moments for image analysis," in *Proc. Int. Conf. Imag. Sci., Syst., Technol. (CISST)*, 2001, pp. 23–29.

[12] R. Mukundan, "Some computational aspects of discrete orthonormal moments," *IEEE Trans. Image Process.*, vol. 13, no. 8, pp. 1055–1059, Aug. 2004.

[13] P. T. Yap, R. Paramesran, and S.-H. Ong, "Image analysis by Krawtchouk moments," *IEEE Trans. Image Process.*, vol. 12, no. 11, pp. 1367–1377, Nov. 2003.

[14] J. Zhou, H. Shu, H. Zhu, C. Toumoulin, and L. Luo, "Image analysis by discrete orthogonal Hahn moments," in *Image Analysis and Recognition*. Berlin, Germany: Springer, 2005, pp. 524–531.

[15] B. M. Mahmmod, A. R. Ramli, T. Baker, F. Al-Obeidat, S. H. Abdulhussain, and W. A. Jassim, "Speech enhancement algorithm based on super-Gaussian modeling and orthogonal polynomials," *IEEE Access*, vol. 7, pp. 103485–103504, 2019.

[16] A. C. D. Brinker, "Stable calculation of Krawtchouk functions from triplet relations," *Mathematics*, vol. 9, no. 16, p. 1972, Aug. 2021.

[17] B. M. Mahmmod, S. H. Abdulhussain, M. A. Naser, M. Alsabah, and J. Mustafina, "Speech enhancement algorithm based on a hybrid estimator," *IOP Conf. Ser., Mater. Sci. Eng.*, vol. 1090, no. 1, Mar. 2021, Art. no. 012102. [Online]. Available: https://iopscience.iop.org/article/10.1088/1757-899X/1090/1/012102

[18] C. Camacho-Bello and J. S. Rivera-Lopez, "Some computational aspects of Tchebichef moments for higher orders," *Pattern Recognit. Lett.*, vol. 112, pp. 332–339, Sep. 2018.

[19] S. H. Abdulhussain, A. R. Ramli, S. A. R. Al-Haddad, B. M. Mahmmod, and W. A. Jassim, "On computational aspects of Tchebichef polynomials for higher polynomial order," *IEEE Access*, vol. 5, pp. 2470–2478, 2017.

[20] B. M. Mahmmod, A. M. Abdul-Hadi, S. H. Abdulhussain, and A. Hussien, "On computational aspects of Krawtchouk polynomials for high orders," *J. Imag.*, vol. 6, no. 8, p. 81, Aug. 2020.

[21] K. A. Al-Utaibi, S. H. Abdulhussain, B. M. Mahmmod, M. A. Naser, M. Alsabah, and S. M. Sait, "Reliable recurrence algorithm for high-order Krawtchouk polynomials," *Entropy*, vol. 23, no. 9, p. 1162, Sep. 2021. [Online]. Available: https://www.mdpi.com/1099-4300/23/9/1162

[22] P. T. Yap, R. Paramesran, and S. H. Ong, "Image analysis using Hahn moments," *IEEE Trans. Pattern Anal. Mach. Intell.*, vol. 29, no. 11, pp. 2057–2062, Nov. 2007.

[23] A. K. E. Mizel, "Orthogonal functions solving linear functional differential equations using Chebyshev polynomial," *Baghdad Sci. J.*, vol. 5, no. 1, pp. 143–148, Mar. 2008.

[24] S. H. Abdulhussain, B. M. Mahmmod, M. A. Naser, M. Q. Alsabah, R. Ali, and S. A. R. Al-Haddad, "A robust handwritten numeral recognition using hybrid orthogonal polynomials and moments," *Sensors*, vol. 21, no. 6, p. 1999, Mar. 2021.

[25] A. Daoui, M. Yamni, O. E. Ogri, H. Karmouni, M. Sayyouri, and H. Qjidaa, "New algorithm for large-sized 2D and 3D image reconstruction using higher-order Hahn moments," *Circuits, Syst., Signal Process.*, vol. 39, no. 9, pp. 4552–4577, Sep. 2020.

[26] A. M. Abdul-Hadi, S. H. Abdulhussain, and B. M. Mahmmod, "On the computational aspects of Charlier polynomials," *Cogent Eng.*, vol. 7, no. 1, Jan. 2020, Art. no. 1763553.

[27] H. Zhu, M. Liu, H. Shu, H. Zhang, and L. Luo, "General form for obtaining discrete orthogonal moments," *IET Image Process.*, vol. 4, no. 5, pp. 335–352, Oct. 2010.

[28] S. H. Abdulhussain, A. R. Ramli, B. M. Mahmmod, M. I. Saripan, S. A. R. Al-Haddad, and W. A. Jassim, "A new hybrid form of Krawtchouk and Tchebichef polynomials: Design and application," *J. Math. Imag. Vis.*, vol. 61, no. 4, pp. 555–570, 2019.

[29] I. M. Spiliotis and B. G. Mertzios, "Fast algorithms for basic processing and analysis operations on block-represented binary images," *Pattern Recognit. Lett.*, vol. 17, no. 14, pp. 1437–1450, Dec. 1996.

[30] H. Shu, H. Zhang, B. Chen, P. Haigron, and L. Luo, "Fast computation of Tchebichef moments for binary and grayscale images," *IEEE Trans. Image Process.*, vol. 19, no. 12, pp. 3171–3180, Dec. 2010.

[31] S. H. Abdulhussain and B. M. Mahmmod, "Fast and efficient recursive algorithm of Meixner polynomials," *J. Real-Time Image Process.*, vol. 18, no. 6, pp. 2225–2237, Apr. 2021. [Online]. Available: https://link.springer.com/10.1007/s11554-021-01093-z

[32] S. H. Abdulhussain, A. R. Ramli, B. M. Mahmmod, S. A. R. Al-Haddad, and W. A. Jassim, "Image edge detection operators based on orthogonal polynomials," *Int. J. Image Data Fusion*, vol. 8, no. 3, pp. 293–308, 2017.

[33] R. Koekoek and R. F. Swarttouw, "The Askey-scheme of hypergeometric orthogonal polynomials and its q-analogue," Fac. Tech. Math. Inform., Technische Universiteit Delft, Delft, The Netherlands, Tech. Rep. 98-17, 1996.

[34] J. F. Hart, *Computer Approximations*. Melbourne, FL, USA: Krieger, 1978.

[35] A. K. Jain, *Fundamentals of Digital Image Processing*. Upper Saddle River, NJ, USA: Prentice-Hall, 1989.

BASHEERA M. MAHMMOD received the Ph.D. degree in computer and embedded system engineering from UPM, in 2018. She is currently a Lecturer at the Department of Computer Engineering, University of Baghdad. Her research interests include signal processing, speech enhancement, and computer vision.

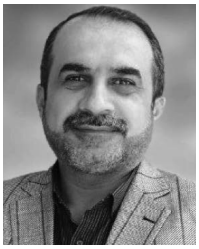

SADIQ H. ABDULHUSSAIN received the Ph.D. degree in computer and embedded system engineering from UPM, in 2018. Since 2008, he has been a Faculty Member with the University of Baghdad. His research interests include image processing, computer vision, and signal processing.

TOMÁŠ SUK (Member, IEEE) received the M.Sc. degree in electrical engineering from the Faculty of Electrical Engineering, Czech Technical University in Prague, Czech Republic, in 1987, the Ph.D. degree in computer science from the Czechoslovak Academy of Sciences, in 1992, and the D.Sc. degree from the Czech Academy of Sciences, Prague, in 2018. Since 1991, he has been a Researcher with the Institute of Information Theory and Automation, Czech Academy of Sciences. He has authored more than 35 journal articles and more than 50 conference papers. He has coauthored the Monographs *Moments and Moment Invariants in Pattern Recognition*. His research interests include invariant features, pattern recognition, image filtering, digital image processing, and moment-based and point-based invariants.

ABIR HUSSAIN (Member, IEEE) is currently a Professor of machine learning with the Department of Computer Science, Liverpool John Moores University. Her research interests include machine learning algorithms and their applications to medical, image and signal processing, and data analysis.